Group A *Streptococcus* Induces Lysosomal Dysfunction in THP-1 Macrophages

Scott T. Nishioka[1†], Joshua Snipper[1†], Jimin Lee[1], Joshua Schapiro[1], Robert Z. Zhang[1], Hyewon Abe[1], Andreas Till[2,3], Cheryl Y.M. Okumura[1*]

[1]Biology Department, Occidental College, Los Angeles, CA 90041, USA

[2]Division of Biological Sciences and The San Diego Center for Systems Biology, University of California San Diego, La Jolla, CA 92093-0688, USA

[3]University Hospital of Bonn, Bonn, Germany

[†]These authors have contributed equally to this work and share first authorship

*** Correspondence:**
Cheryl Okumura
okumura@oxy.edu

Keywords: Group A *Streptococcus*, streptolysin O (SLO), macrophage, lysosome, vacuolar ATPase, cathepsin B

Abstract

The human-specific bacterial pathogen Group A *Streptococcus* (GAS) is a significant cause of morbidity and mortality. Macrophages are important to control GAS upon infection, but previous data indicate that GAS can persist in macrophages. In this study, we detail the molecular mechanisms by which GAS survives in THP-1 macrophages. Our fluorescence microscopy studies demonstrate that GAS are readily phagocytosed by macrophages, but persist within phagolysosomes. These phagolysosomes are not acidified, which is in agreement with the inability of the GAS to survive in low pH environments. We find that the secreted pore-forming toxin Streptolysin O (SLO) perforates the phagolysosomal membrane, allowing leakage of not only protons, but large proteins including the lysosomal protease cathepsin B. Additionally, GAS blocks the activity of vacuolar ATPase (v-ATPase) to prevent acidification of the phagolysosome. Thus, while GAS does not inhibit fusion of the lysosome with the phagosome, it has multiple mechanisms to prevent proper phagolysosome function, allowing for persistence of the bacteria within the macrophage. This has important implications for not only the initial response, but the overall function of the macrophages and resulting pathology in GAS infection and suggests that therapies aimed at improving macrophage function may improve outcomes in GAS infection.

1 Introduction

GAS is a significant cause of morbidity and mortality worldwide, but especially in medically underserved areas where antibiotic therapy may not be promptly available (1). Infection produces wide-ranging clinical manifestations including pharyngitis, acute rheumatic fever (ARF) often leading to rheumatic heart disease, and invasive disease such as necrotizing fasciitis (1). Acting as the first line of defense against such infections, macrophages are critical for the early control and resolution of GAS infection (2,3). However, GAS has been shown to survive intracellularly in macrophages during both acute invasive soft tissue infection and asymptomatic carriage (3–5). Although GAS remains highly sensitive to beta-lactam antibiotics, the gold standard of treatment (6),

the ability of bacteria to persist in macrophages and re-emerge after antibiotic treatment poses a therapeutic challenge (4).

As both phagocytes and antigen-presenting cells, macrophages function at the intersection of innate and adaptive immunity and are therefore critical for identifying and defending against infection. Macrophages engulf bacterial pathogens into phagosomes, which fuse with lysosomes that deliver proteolytic enzymes to facilitate bacterial destruction. These enzymes have optimal proteolytic activity under acidic conditions, and therefore lysosomal acidification is important for macrophage bactericidal function and subsequent antigen presentation (7). Inhibition of either lysosomal fusion with bacteria-containing phagosomes or phagolysosomal acidification is an evasion tactic employed by several bacterial pathogens including *Mycobacterium tuberculosis*, *Legionella pneumophila*, and *Staphylococcus aureus* (7–9). GAS may employ similar tactics to survive intracellularly within macrophages and to evade the adaptive immune response upon host re-infection, which may contribute to the development of pathologies such as toxic shock syndrome (10).

GAS is a human-specific pathogen and therefore has evolved mechanisms to survive the immune response (11). Previous data have indicated that phagocytosed GAS can prevent fusion with destructive organelles such as azurophilic granules and lysosomes (12,13). Other reports have shown that while GAS-containing phagosomes do fuse with lysosomes, GAS survives within macrophages via the secretion of virulence factors such as Streptolysin O (SLO) and NADase (14,15). SLO is a cholesterol-dependent cytolysin that oligomerizes to form large pores (~25-30 nm) within the host cell membrane (16). As a result, SLO is hypothesized to permeabilize the phagolysosomal membrane, permitting free flow of protons out of the phagolysosome and limiting the activity of lysosomal proteases that facilitate intracellular killing (15,17). Interestingly, it has also been reported that GAS is capable of preventing lysosomal acidification by preventing the recruitment of the vacuolar ATPase (v-ATPase) (18). In the context of these data, it is unclear what mechanisms are contributing to GAS intracellular survival in macrophages. In this paper, we used the human monocytic cell line THP-1 differentiated into macrophages to understand the molecular mechanism by which GAS survives in macrophages. We find that not only does GAS induce leakage of large proteins from the phagolysosome into the cytosol, but that acidification of the phagolysosome is also limited. This has important consequences for the survival of the bacteria within the macrophage and underscores the need to mount a proper macrophage response in GAS infection to improve patient outcomes.

2 Materials and Methods

2.1 Antibodies and chemicals

Antibodies to the following proteins were used in this study: EEA-1 (Abcam, ab2900), LAMP-2 (Abcam, ab25631), V_0D_1 (Abcam, ab56441), Cathepsin B (Cell Signaling Technology, D1C7Y), LAMP-1 (Cell Signaling Technology, #9091), V_1A (Abnova, H00000523-A01), and beta-actin (Thermo Fisher Scientific, MA5-15739). Fluorescent secondary antibodies were purchased from Thermo Fisher Scientific. The following fluorescent probes were purchased from Thermo Fisher Scientific: Alexa Fluor 488 Hydrazide (A10436), Oregon Green 488 Anionic, Lysine Fixable Dextran,10,000 MW (D7171) and 70,000 MW (D7173), and LysoTracker DeepRed (L12492). 40,000 and 70,000 MW Fluorescein isothiocyanate (FITC) dextrans were purchased from Millipore Sigma. To generate antibody-coupled beads, 0.1um Carboxylate-Modified Microspheres (Thermo Fisher Scientific) were coupled to approximately 400mg normal pooled human serum (Thermo

Fisher Scientific) using 2% 1-Ethyl-3-(3-dimethylaminopropyl) carbodiimide hydrochloride (QBiosciences). The reaction was quenched with 40mM ethanolamine and resuspended in PBS. Successful coupling of the beads was assessed by fluorescence microscopy and increased phagocytosis by THP-1 macrophages compared with uncoupled beads (data not shown). 1mM L-leucyl L-leucine O-methyl ester (LLOMe, Cayman Chemical, #16008) was incubated with cells to induce lysosomal damage.

2.2 Bacterial strains

Wild-type (WT) GAS strain M1T1 5448 (M1 GAS) was originally isolated from a patient with necrotizing fasciitis and toxic shock syndrome (19). Isogenic mutant strains lacking Streptolysin O (ΔSLO), Streptolysin S (via lack of SagA, ΔSagA) and Emm1 (ΔM1) were previously described (20–22). Bacterial strains were cultivated in Todd-Hewitt broth (THB) at 37˚C. For all experiments, bacteria were grown to log phase in the presence of 1:200 pooled normal human serum (Thermo Fisher Scientific) to opsonize bacteria. The gene for monomeric WASABI (mWASABI) (23,24) was codon-optimized for expression in bacteria and synthesized in a shuttle vector (GenScript; see supplemental data for amino acid sequence). The gene was subcloned into pDCerm (25) and the resulting plasmid (pWASABI) was transformed into WT M1 GAS and the ΔSLO mutant. Plasmid-bearing strains were maintained in THB supplemented with 5ug/mL erythromycin. Heat-killed (HK) bacteria were prepared by incubating a known concentration of bacteria at 95°C for 10 min. followed by a 15 min. opsonization in 1:200 pooled normal human serum at room temperature.

2.3 Cell Culture

THP-1 cells were purchased from Sigma (cat. 88081201) and cultured in RPMI supplemented with 10% heat inactivated fetal bovine serum (FBS) (Corning), 2mM L-glutamine and 100 U/mL penicillin/100 µg/mL streptomycin at 37°C/5% CO_2. Cells were differentiated to macrophages using 20nM phorbol 12-myristate 13-acetate (PMA) (MilliporeSigma) 24-48 hours prior to experiments.

2.4 Immunofluorescence

2.5 x 10^5 THP-1 cells were seeded on coverslips in the presence of 20nM PMA 24-48 hours prior to experiments. For dextran leakage assays, cells were incubated in media containing 20ug/mL of the indicated dextran or 500ug/mL 70kD dextran overnight, washed and chased in cell culture media for 2 hours prior to bacterial infection. Bacteria were combined with cells at an MOI = 10 in RPMI supplemented with 2% FBS only (no antibiotics). At the indicated time points, cells were fixed with 4% paraformaldehyde or 3.7% formaldehyde for 10 min. at room temperature. Cells were incubated with blocking solution (10% goat serum, 3% BSA and 0.1% Triton X-100 in PBS), then incubated with the indicated primary antibodies for 1 hour at room temperature in block solution. Cells were washed and incubated with the indicated secondary antibodies for 1 hour at room temperature. Cells were washed and mounted onto slides with ProLong antifade reagent with DAPI (Thermo Fisher Scientific). Slides were imaged on an inverted Leica TCS SP5 confocal microscope using a 63x/1.40 oil objective with 2-3x digital zoom at calibrated magnifications and recorded with LAS AF software (Leica). Quantitation of dextran and LAMP-1 colocalization with bacteria was analyzed with CellProfiler 3.1.9 (26) using the Otsu thresholding method. For dextran, colocalization is expressed as the percentage of dextran-labeled lysosomes that colocalized with bacteria compared with the total number of lysosomes. For LAMP-1, colocalization is expressed as the percentage of LAMP-1 that colocalized with bacteria compared with the total number of bacteria. For quantitation of GFP-expressing bacteria within phagosomes, images were coded and counted manually in a blind fashion by at least 4 independent reviewers. For all imaging data, at least 3 independent experiments were

performed, at least 16 images containing >10 cells per image were analyzed and at least 100 cells were counted per time point.

2.5 Verification of pH sensitivity of mWASABI in GAS

To assess the fluorescence intensity of mWASABI in live GAS, log phase cultures of bacteria were incubated on coverslips in THB with 10mM HEPES adjusted to the indicated pH for 1 hour at 37°C. Bacteria were fixed with 2% paraformaldehyde and analyzed by confocal microscopy. Gain settings were adjusted to bacteria incubated in pH 7 media, and the same settings were applied to all other conditions. Images were thresholded and the corrected total cell fluorescence (integrated density – average background integrated density) of each bacterial cell was measured using ImageJ.

2.6 Acidification assay

10^5 THP-1 cells were seeded with 20nM PMA in 96-well black plates with clear bottoms overnight. Cells were fed 500ug/mL 70kD FITC-dextran overnight. The following day, cells were chased with normal cell culture media for 2 hours prior to infection. Cells were infected at an MOI of 10 with either the indicated bacterial strain or Ab-conjugated latex beads. Fluorescence intensity at 480nm/535nm (Em/Ex) was monitored at 37°C in a fluorescent plate reader every 15 min. for 3 hours.

2.7 Bacterial survival in different pH media

Bacteria were incubated in THB with 10mM HEPES adjusted to the indicated pH. For bacterial growth, cultures were adjusted to an OD_{600nm} of 0.1 and incubated at 37°C. OD_{600nm} was measured every 15 min. For bacterial survival, 2 x 10^5 cfu log phase bacteria were added to 250ul pH-adjusted culture media in 96 well plates. At the indicated time point, a 25ul aliquot was removed from the culture and quantitated by plating on agar plates.

2.8 Cell fractionation and Western blot

Following a 30 min. infection period, a total of 10^7 PMA-differentiated cells were scraped and collected in 1 mL of fractionation buffer (50 mM KCl, 90 mM K-Gluconate, 1 mM EGTA, 5 mM MgCl2, 50 mM sucrose, 20 mM HEPES, pH 7.4, 5 mM glucose, 1X HALT phosphatase/protease inhibitor cocktail (Thermo Fisher Scientific), 1ug/mL pepstatin (Millipore Sigma), and 1mM PMSF (Millipore Sigma)). Cells were lysed by nitrogen cavitation equilibrated on ice for 30 min. at 400 psi. The resulting lysates were fractionated into membrane and cytosolic fractions by centrifugation at 16,000 xg at 4˚C for 15 min. (pellet = membrane fraction, supernatant = cytosolic fraction). Protein concentrations were measured by BCA assay (Thermo Fisher Scientific). 10ug of each sample was run on SDS-PAGE gels and transferred to a 0.2um PVDF membrane. Blots were blocked with 5% (w/v) non-fat dry milk in 1X Tris-buffered saline with 0.1% Tween 20 (TBST). Blots were probed with the indicated antibodies overnight at 4˚C. Relative protein concentrations were quantified by densitometry analysis in ImageLab v. 6.0.1 (BioRad). v-ATPase assembly was measured by normalizing V_1A densitometry values in the membrane fraction to the V_0D_1 loading controls (in membrane fractions) and calculating the ratio of V_1A in the sample compared with uninfected macrophages (27).

2.9 Cathepsin B activity assay

4 x 10^6 PMA-differentiated THP-1 cells were infected at an MOI = 10 for 60 min. followed by lysis with 30ug/mL digitonin in acetate buffer (50 mM Na-acetate pH 5.6, 150 mM NaCl, 0.5 mM EDTA)

and protease inhibitors (1X HALT phosphatase/protease inhibitor cocktail (Thermo Fisher Scientific), 100 μM PMSF, 1 μg/mL pepstatin)) (28). The cell lysate was separated into cytosolic and membrane fractions as described above. Cathepsin B activity in cytosolic fractions was measured using the SensoLyte 520 Cathepsin B Assay Kit (AnaSpec) according to the manufacturer's instructions. Relative fluorescence units were normalized to the corresponding protein concentration for each sample and compared with the untreated cells. Data from 3 independent experiments were combined.

2.10 v-ATPase activity assay

Cell membrane fractions containing lysosomes were prepared using 30ug/mL digitonin in acetate buffer as described above. 10ug of each sample was equilibrated in 200ul assay buffer (10mM HEPES, 5mM MgCl2, 125mM KCl, pH = 7.0) (29) at room temperature for 30 min. in the presence or absence of 200nM bafilomycin (MilliporeSigma). 1mM fresh ATP in 200mM Tris pH = 7 was added to each sample and incubated at room temperature for 2.5 hours. 25ul of the reaction was collected and diluted in ultrapure water, and liberation of free phosphate was measured using the Malachite Green Phosphate Assay Kit according to the manufacturer's instructions (MilliporeSigma). Corrected absorbance values (= A_{sample} - $A_{substrate\ blank}$ - $A_{buffer\ blank}$) were compared with a phosphate standard curve to determine phosphate concentration. v-ATPase activity was calculated as the difference in phosphate concentration between samples incubated with and without bafilomycin.

2.11 Statistical analysis

Growth curve data was analyzed using the Growthcurver package in R (30) and comparison of the intrinsic growth rate (r) and carrying capacity (K) was analyzed by one-way ANOVA and Tukey's post-hoc test. All other data were analyzed using Prism v. 9.3.1 (GraphPad Software) by one-way ANOVA with Tukey's (normally distributed data) or Kruskal-Wallis (nonparametric data) multiple comparison tests. Outliers were assessed by the ROUT method (Q = 1%). For all data presented, ****P<0.0001, ***P<0.001, *P<0.05, n.s., not significant.

3 Results

3.1 Bacterial trafficking in THP-1 macrophages

We first wanted to determine the intracellular fate of GAS in THP-1 macrophages. To study bacterial trafficking, we performed a short time course infection experiment with WT M1 GAS and tracked phagolysosomal maturation. In agreement with other reports (13,15,31), bacteria were rapidly engulfed by THP-1 cells within 7.5 minutes (Fig. 1A, B) and colocalized with the phagolysosomal marker EEA-1 (Fig. 2). Interestingly, bacteria in phagosomes began colocalizing with the lysosomal marker LAMP-1 as early as 7.5 minutes, with maximal colocalization at 30 minutes (Fig. 1A, B). GAS remained in phagolysosomes throughout the later time points (Fig. 1B), and the number of bacteria per cell was relatively constant throughout the experiment (Fig. 1C). These data indicated that bacteria were trafficked normally to phagolysosomes, but bacteria were held in these compartments without observable bacterial killing.

3.2 GAS reside in non-acidified phagolysosomes in THP-1 macrophages

Because bacteria appeared to be held in phagolysosomes, we wondered whether phagolysosomes containing GAS were acidified. Acidification is critical for optimal activity of the proteolytic enzymes in the lysosome (32). Lysotracker is an acidotropic dye commonly used to track

acidic compartments such as lysosomes in the cell. However, because GAS is an acid-producing bacterial species, we tested whether Lysotracker would be an accurate indicator of lysosomal pH in GAS-infected cells. Although Lysotracker colocalized with lysosomal markers in THP-1 cells, the staining and uptake was inconsistent (Supp. Fig. 1A). Furthermore, bacteria were brightly stained with Lysotracker in both infected cells and in the absence of cells (Supp. Fig. 1A-C). This made it difficult to determine whether and to what extent phagolysosomes containing GAS were acidified. We therefore expressed a pH-sensitive green fluorescent protein variant mWASABI (24) in GAS to monitor phagolysosomal pH of GAS-infected cells (Fig. 2A). Green fluorescence produced by live bacteria was appropriately quenched in low pH environments (Fig. 2A, B). Notably, pH was distinguishable by fluorescence intensity between pH 5.0 and 4.5 (Fig. 2B).

We infected THP-1 macrophages with mWASABI-expressing GAS and performed a detailed trafficking assay of GAS through the phagolysosomal pathway (Fig. 2C, D). Because bacteria were tracked by mWASABI expression instead of immunofluorescent staining, we manually counted bacteria that colocalized with phagolysosomal markers (Fig. 2C, D). We again found that GAS was initially located in phagosomes, as indicated by EEA-1 staining, which was followed by rapid bacterial colocalization with the mature lysosomal marker LAMP-2 within 15 minutes of infection (Fig. 2C, D), similar to the colocalization dynamics observed with LAMP-1 staining (Fig. 1). A significant proportion of the total intracellular bacteria were colocalized with LAMP-2 within 60 minutes post-infection (Fig. 2C, D). Although there were some fluctuations in the number of bacteria in phagolysosomes (Fig. 2E), the number of intracellular bacteria remained relatively constant at all time points, consistent with our initial data (Fig. 1C). This corroborated our finding that little to no bacterial eradication or replication was occurring within this time frame (Fig. 2E). Surprisingly, we also found that the green fluorescence signal did not diminish over time (Fig. 2C, F). Fluorescence signal intensity of intracellular bacteria in phagolysosomes was not significantly different than that of extracellular bacteria (Fig. 2F). As the lysosomal lumen is typically between pH 4.5–5 when acidified (33), a pH level that our mWASABI probe can differentiate (Fig. 2A, B), these data indicated that GAS were maintained in phagolysosomes that are not appropriately acidified.

We confirmed that GAS-infected phagosomes were not acidified with a second method using pH-sensitive FITC-conjugated 70kD dextran particles. Acidification of the lysosomes resulted in quenching of the fluorescence signal in uninfected and control cells infected with immunoglobulin-conjugated beads (Fig. 2G). However, the fluorescence signal was increased in cells infected with all tested strains of GAS, indicating no pH change (Fig. 2G). These results confirmed that GAS-infected phagolysosomes are not properly acidified, which may account for the persistence of the bacteria in THP-1 cells (Fig. 1C, 2E).

3.3 GAS does not tolerate lysosomal acidic conditions

The pH of the lysosomal lumen has been reported to range between pH 4.5-5 (33). Because GAS is a lactic acid-producing bacterial species capable of acidifying its environment and possesses systems such as the arginine deiminase (ADI) pathway that confer acid tolerance (34,35), we wondered whether a pH similar to that found in the lysosome adversely affected bacterial growth and survival. In growth experiments, bacteria grown in media adjusted to pH 5 or lower did not demonstrate measurable growth (Fig. 3A). Bacteria grown in media adjusted to pH 6 grew at a significantly slower rate and did not reach a similar maximum population size in the time frame of our experiment compared with the unbuffered media control (Fig. 3A). Although growth rates were slower, the ability of bacteria to grow in pH 6 media is consistent with the ability of bacteria to grow in increasingly acidified media, as indicated by the final pH of the stationary phase cultures in

unbuffered culture media (Table 1). For bacteria grown in buffered media adjusted to pH 7, there was no significant difference in maximum population size, but a statistically significant increase in the intrinsic growth rate of the population compared with unbuffered media (Fig. 3A). Thus, bacterial growth is inhibited by low pH. As expected, we found that the final pH of both buffered and unbuffered culture medium after bacterial growth was acidic (Table 1).

Quantitative plating of cultures at various time points throughout the growth experiment indicated that bacteria in pH 5 media were present, but not measurably growing (data not shown). We therefore performed a detailed time course to monitor bacterial survival in low pH media (Fig. 3B). Bacteria incubated in unbuffered media did not significantly grow during the time frame of the experiment (data not shown). Similar to other studies (36,37), we found that GAS does not survive in low pH media (Fig. 3B). Although bacteria incubated in up to pH 5.3 media could survive for a short time, bacterial numbers declined at later time points (Fig. 3B), in agreement with pH 5 being the limit at which bacteria can survive (35,38) and the final pH of bacteria grown in media (Table 1). Combined, our data affirm that GAS cannot survive in the acidified lysosome. Thus, in order to persist in the phagolysosome, GAS likely prevents its acidification.

3.4 Streptolysin O creates large perforations in the phagolysosome

Although GAS has several acid stress response strategies, a better tactic may be to avoid the acidification of the phagolysosome altogether (39). The inability of bacteria to survive in low pH environments (Fig. 3) led us to examine whether GAS infection has a mechanism to prevent phagolysosomal acidification. Pore-forming toxins such as SLO create pores as large as 25-30nm in size (16). Streptolysin S (SLS) can similarly perforate membranes (40). Others have shown that pore-forming toxins, including SLO, allow escape of hydrogen ions that prevent acidification of the lysosome (15,41). To confirm these data, we fed THP-1 macrophages fluorescent-conjugated molecules and dextrans of various sizes to assess pore size and leakage from phagolysosomes in GAS-infected cells. The ability to measure phagosomal leakage was confirmed using a fluorescent dye approximately 570Da in size, a 10kD dextran and the lysosomal permeabilization agent LLOMe (Supp. Fig. 2A). LLOMe permeabilizes lysosomes to molecules up to at least 4.4KDa, but not to molecules greater than 10kD (28). Retention of the 10kD, but not the 570Da probe in LLOMe-treated cells confirmed uptake of the probe in phagolysosomes and appropriate release into the cytosol upon permeabilization (Supp. Fig. 2A). Cells loaded with probes were infected with various strains of GAS (Fig. 4A, B). As expected, WT GAS caused probes up to 40kD in size, approximately 9nm diameter (42), to leak from phagolysosomes (Fig. 4A, B). ΔSLO GAS-infected cells retained the probes, while cells infected with ΔSagA GAS (lacking SLS) allowed leakage of the probes, similar to the WT strain (Fig. 4A, B). Mutant bacteria lacking the surface protein M1 (ΔM1), but with unaltered expression of SLO and SLS behaved similarly to WT strains (Fig. 4A, B). Heat-killed bacteria (HK) that retain surface structure but are unable to secrete proteins such as SLO and SLS were included as a comparison and corroborated the data from cells infected with the live GAS strains (Fig. 4A, B). Compared with heat-killed bacteria, WT bacteria could retain probes up to 70kD in size (approximately 13nm diameter) in agreement with the literature (42), though it is possible that leakage of probes of this size still occurs (Fig. 4B, compare with ΔSLO). In our assays, SLS did not significantly damage the phagolysosomal membrane, as indicated by the lack of leakage of even the small 570Da probe (Supp. Fig. 2B). These data indicate that SLO is the primary pore-forming toxin that perforates the phagolysosome and allows leakage of not only protons, but relatively large molecules.

Because such large molecules can leak from GAS-infected phagosomes, we wondered whether lysosomal enzymes could escape into the cytosol through SLO-mediated pores. We infected cells with WT or ΔSLO GAS and collected membrane and cytosolic cell fractions. Lack of lysosomal markers in the cytosolic fraction indicated little to no contamination of the cytosolic fraction with lysosomes (Fig. 2C). The membrane fraction contained the majority of the lysosomal enzyme cathepsin B as expected (Fig. 2C). However, we noted a small, but visible increase in the amount of cathepsin B present in the cytosolic fraction of WT-infected cells compared with uninfected and ΔSLO-infected cells (Fig. 2C). In order to verify that cathepsin B was present in the cytosol, we measured cathepsin B activity in the cytosolic fraction. Cytosolic fractions from WT-infected cells contained the highest amount of cathepsin B activity compared with uninfected cells (Fig. 2D). Cytosolic fractions from ΔSLO bacteria incapable of leaking large proteins from the phagolysosome (Fig. 2B) did not exhibit cathepsin B activity higher than background levels in uninfected cells (Fig. 2D). These data confirmed that SLO secreted by WT bacteria perforates the phagolysosomal membrane and allows the leakage of large proteins into the cytosol. This loss of proteolytic enzymes from the phagolysosome likely also contributes to the ability of GAS to persist in the phagolysosome during infection.

3.5 GAS prevents proper function of vacuolar ATPase

Although SLO-mediated pores could cause leakage of protons from the phagolysosome, reports in the literature suggest that the v-ATPase that is required for acidification of the lysosome is non-functional in GAS-infected cells (18). Supporting this, we found that the phagolysosomes of macrophages infected with ΔSLO and heat-killed bacteria were also not acidified (Fig. 2G). Furthermore, ΔSLO bacteria are trafficked to phagolysosomes and are maintained at consistent numbers in THP-1 cells similar to WT bacteria (Supp. Fig. 3), consistent with the idea that phagolysosomes infected with ΔSLO bacteria were not acidified. We therefore investigated whether v-ATPase is properly assembled and functional in GAS-infected cells. v-ATPase consists of the membrane-bound F_0 subunit (containing the V_0D_1 protein) that must assemble with the cytosolic F_1 subunit (containing the V_1A) for proper function (27). We monitored v-ATPase assembly by tracking movement of the V_1A subunit from the cytosolic to membrane fractions. Cells fed Ig-conjugated beads (Ab beads) were included as a positive control (Fig. 5A, B). We observed no significant difference in v-ATPase subunit assembly in cells infected with GAS compared to Ab-bead fed or uninfected cells (Fig. 5A, B). This observation was consistent for cells infected with either WT or ΔSLO GAS, as well as heat-killed bacteria (Fig. 5A, B). However, when we measured the v-ATPase activity in membrane fractions of GAS-infected cells, we found significantly decreased v-ATPase activity in fractions from cells infected with all strains of GAS compared with uninfected cells (Fig. 5C). These data are in agreement with the lack of acidification in GAS-infected cells (Fig. 2G). Therefore, though the v-ATPase is properly assembled in GAS-infected cells, the activity of this enzyme is decreased, preventing proper acidification of the phagolysosome. Thus, our data suggests that GAS persists in macrophages by employing a multi-pronged approach to avoid the destructive mechanisms of the phagolysosome.

4 Discussion

The human-specific pathogen GAS has co-evolved with the human immune system, and therefore has multiple mechanisms for survival within the host (1,11). Although GAS is an extracellular bacterial pathogen, phagocytic cells such as macrophages can readily engulf bacteria (13,15,31). The ability of GAS to not only survive in macrophages, but to potentially alter their

function, escape downstream immune responses, and be sheltered from antibiotic treatment provides a basis for successful persistence in humans.

In our experiments, we found that GAS was readily phagocytosed and phagosomes quickly fused with lysosomes, but that GAS remained intact in these compartments (Fig. 1, 2). There is conflicting evidence in the literature about the fusion of lysosomes with GAS-containing phagosomes in macrophages, which may be due to a difference in cell origin or antibodies (13,15). In addition, we corroborated previous data that SLO induces perforation and damage of the phagolysosomal membrane (Fig. 4) (15,43). Although ΔSLO GAS also prevented phagolysosomal acidification (Fig. 2, 5), others have shown that ΔSLO GAS are less fit for survival in macrophages and other cells (15,44). ΔSLO GAS is likely still susceptible to other macrophage killing mechanisms such as reactive oxygen species or xenophagy (44). However, all data are in agreement that in macrophages, GAS does not escape into the cytosol and remains in a membrane-bound structure (Fig. 2, Supp. Fig. 3) (13,15). In THP-1 macrophages, bacteria do not replicate in this structure, but they are also not eradicated (Fig. 1, 2, Supp. Fig. 3) (31). This is different from what has previously been observed in epithelial cells, where GAS escapes into the cytosol and replicates (14,43). The downstream fate of GAS in non-functional lysosomes in THP-1 macrophages remains to be elucidated.

The pH of the lysosomal lumen has been reported to range between pH 4.5-5 (33). However, we found that acidified medium was sufficient to kill GAS (Fig. 3). These results are surprising since not only does GAS produce lactic acid, but previous reports suggest GAS has multiple mechanisms for acid tolerance, including a F_0/F_1 proton pump and the arginine deiminase pathway which produces alkali (34,35,39,45). However, there may be a limit to which these systems work, especially within an enclosed environment such as in vitro conditions or in the phagolysosome, as demonstrated by the threshold for bacterial survival in low pH medium (Fig. 3) (35). Additionally, GAS lacks enzymes such as glutamate decarboxylase and urease (39), making neutralization of highly acidified environments a less viable strategy. Therefore, two mechanisms to prevent acidification, perforating the phagolysosomal membrane (Fig. 4) and blocking v-ATPase activity (Fig. 5) provide a means to survive within the phagolysosomal compartment. Other bacteria such as *Legionella pneumophila* have proteins such as SidK, which binds v-ATPase subunits to prevent activity (29). Our data indicate that neither SLO nor any other secreted factor is responsible for interfering with v-ATPase activity (Fig. 5c), and the identity of the responsible GAS protein(s) remains to be elucidated.

Previous data and our results indicate SLO causes leakage of lysosomal contents (Fig. 4). These proteins include active lysosomal enzymes such as cathepsin B (Fig. 4) but could also include bacteria proteases such as SpeB, whose presence in the cytosol could lead to NLRP3 inflammasome activation and release of the proinflammatory cytokine IL-1β (46–50). Persistent IL-1β activation as a result of GAS infection has been linked with ARF and rheumatic heart disease (51). Thus, besides enabling bacterial survival and blunting the normal macrophage response, the resulting macrophage response may lead to pathologies such as ARF that are observed during GAS infection. Furthermore, SLO promotes macrophage apoptosis by releasing SLO from the lysosome and causing mitochondrial damage (20,52). Loss of macrophages may also have detrimental effects on the long-term response to GAS infection, including the inability to generate protective antibodies. Therapies aimed at improving macrophage function may therefore improve GAS infection outcomes. Although SLO is a promising target, our work shows that additional drugs to restore v-ATPase activity would be necessary to restore macrophage function.

5 Conflict of Interest

The authors declare that the research was conducted in the absence of any commercial or financial relationships that could be construed as a potential conflict of interest.

6 Author Contributions

SN, JS, AT and CO contributed to conception and design of the study. All authors performed the experiments and analyzed data. CO wrote the first draft of the manuscript. All authors contributed to manuscript revision, read, and approved the submitted version.

7 Funding

Support for this project has been provided by the American Heart Association (17GRNT33410851 to CO), the Fletcher Jones Science Scholars Fellowship (to SN), the Occidental College Undergraduate Research Center (to SN, JS, JL, JS, RZ and HA), Occidental College (to CO) and the San Diego Center for Systems Biology (to AT).

8 Acknowledgments

We thank Cheldon Alcantara and Ryan Hino for contributions to experiments, and Kelvin Zheng, Jessica Kim, Stephanie Peacock, Isabel Perez, Kevin Kim, and the Fall 2021 Bio 395 GRR course for contributions to data analysis in this paper.

9 References

1. Sims Sanyahumbi A, Colquhoun S, Wyber R, Carapetis JR. Global Disease Burden of Group A Streptococcus. In: Ferretti JJ, Stevens DL, Fischetti VA, editors. Streptococcus pyogenes : Basic Biology to Clinical Manifestations [Internet]. Oklahoma City (OK): University of Oklahoma Health Sciences Center; 2016 [cited 2022 Apr 11]. Available from: http://www.ncbi.nlm.nih.gov/books/NBK333415/

2. Goldmann O, Rohde M, Chhatwal GS, Medina E. Role of Macrophages in Host Resistance to Group A Streptococci. Infect Immun. 2004 May;72(5):2956–63.

3. Mishalian I, Ordan M, Peled A, Maly A, Eichenbaum MB, Ravins M, et al. Recruited macrophages control dissemination of group A Streptococcus from infected soft tissues. J Immunol Baltim Md 1950. 2011 Dec 1;187(11):6022–31.

4. Thulin P, Johansson L, Low DE, Gan BS, Kotb M, McGeer A, et al. Viable group A streptococci in macrophages during acute soft tissue infection. PLoS Med. 2006 Mar;3(3):e53.

5. Österlund A, Popa R, Nikkilä T, Scheynius A, Engstrand L. Intracellular Reservoir of Streptococcus pyogenes In Vivo: A Possible Explanation for Recurrent Pharyngotonsillitis. The Laryngoscope. 1997;107(5):640–7.

6. Johnson AF, LaRock CN. Antibiotic Treatment, Mechanisms for Failure, and Adjunctive Therapies for Infections by Group A Streptococcus. Front Microbiol. 2021;12:760255.

7. Flannagan RS, Heit B, Heinrichs DE. Antimicrobial Mechanisms of Macrophages and the Immune Evasion Strategies of Staphylococcus aureus. Pathogens. 2015 Dec;4(4):826–68.

8. Carranza C, Chavez-Galan L. Several Routes to the Same Destination: Inhibition of Phagosome-Lysosome Fusion by Mycobacterium tuberculosis. Am J Med Sci. 2019 Mar;357(3):184–94.

9. Misch EA. Legionella: virulence factors and host response. Curr Opin Infect Dis. 2016 Jun;29(3):280–6.

10. Ganem MB, De Marzi MC, Fernández-Lynch MJ, Jancic C, Vermeulen M, Geffner J, et al. Uptake and intracellular trafficking of superantigens in dendritic cells. PloS One. 2013;8(6):e66244.

11. Siemens N, Snäll J, Svensson M, Norrby-Teglund A. Pathogenic Mechanisms of Streptococcal Necrotizing Soft Tissue Infections. Adv Exp Med Biol. 2020;1294:127–50.

12. Staali L, Bauer S, Mörgelin M, Björck L, Tapper H. Streptococcus pyogenes bacteria modulate membrane traffic in human neutrophils and selectively inhibit azurophilic granule fusion with phagosomes. Cell Microbiol. 2006 Apr;8(4):690–703.

13. Hertzén E, Johansson L, Wallin R, Schmidt H, Kroll M, Rehn AP, et al. M1 protein-dependent intracellular trafficking promotes persistence and replication of Streptococcus pyogenes in macrophages. J Innate Immun. 2010;2(6):534–45.

14. Walker MJ, Barnett TC, McArthur JD, Cole JN, Gillen CM, Henningham A, et al. Disease Manifestations and Pathogenic Mechanisms of Group A Streptococcus. Clin Microbiol Rev. 2014 Apr 1;27(2):264–301.

15. Bastiat-Sempe B, Love JF, Lomayesva N, Wessels MR. Streptolysin O and NAD-glycohydrolase prevent phagolysosome acidification and promote group A Streptococcus survival in macrophages. mBio. 2014 Sep 16;5(5):e01690-01614.

16. Bhakdi S, Tranum-Jensen J, Sziegoleit A. Mechanism of membrane damage by streptolysin-O. Infect Immun. 1985 Jan;47(1):52–60.

17. Håkansson A, Bentley CC, Shakhnovic EA, Wessels MR. Cytolysin-dependent evasion of lysosomal killing. Proc Natl Acad Sci U S A. 2005 Apr 5;102(14):5192–7.

18. Nordenfelt P, Grinstein S, Björck L, Tapper H. V-ATPase-mediated phagosomal acidification is impaired by Streptococcus pyogenes through Mga-regulated surface proteins. Microbes Infect. 2012 Nov;14(14):1319–29.

19. Chatellier S, Ihendyane N, Kansal RG, Khambaty F, Basma H, Norrby-Teglund A, et al. Genetic relatedness and superantigen expression in group A streptococcus serotype M1 isolates from patients with severe and nonsevere invasive diseases. Infect Immun. 2000 Jun;68(6):3523–34.

20. Timmer AM, Timmer JC, Pence MA, Hsu LC, Ghochani M, Frey TG, et al. Streptolysin O promotes group A Streptococcus immune evasion by accelerated macrophage apoptosis. J Biol Chem. 2009 Jan 9;284(2):862–71.

21. Lauth X, von Köckritz-Blickwede M, McNamara CW, Myskowski S, Zinkernagel AS, Beall B, et al. M1 protein allows Group A streptococcal survival in phagocyte extracellular traps through cathelicidin inhibition. J Innate Immun. 2009;1(3):202–14.

22. Datta V, Myskowski SM, Kwinn LA, Chiem DN, Varki N, Kansal RG, et al. Mutational analysis of the group A streptococcal operon encoding streptolysin S and its virulence role in invasive infection. Mol Microbiol. 2005 May;56(3):681–95.

23. Ai H wang, Olenych SG, Wong P, Davidson MW, Campbell RE. Hue-shifted monomeric variants of Clavularia cyan fluorescent protein: identification of the molecular determinants of color and applications in fluorescence imaging. BMC Biol. 2008 Mar 6;6:13.

24. Zhou C, Zhong W, Zhou J, Sheng F, Fang Z, Wei Y, et al. Monitoring autophagic flux by an improved tandem fluorescent-tagged LC3 (mTagRFP-mWasabi-LC3) reveals that high-dose rapamycin impairs autophagic flux in cancer cells. Autophagy. 2012 Aug;8(8):1215–26.

25. Jeng A, Sakota V, Li Z, Datta V, Beall B, Nizet V. Molecular genetic analysis of a group A Streptococcus operon encoding serum opacity factor and a novel fibronectin-binding protein, SfbX. J Bacteriol. 2003 Feb;185(4):1208–17.

26. McQuin C, Goodman A, Chernyshev V, Kamentsky L, Cimini BA, Karhohs KW, et al. CellProfiler 3.0: Next-generation image processing for biology. PLoS Biol. 2018 Jul;16(7):e2005970.

27. McGuire CM, Forgac M. Glucose starvation increases V-ATPase assembly and activity in mammalian cells through AMP kinase and phosphatidylinositide 3-kinase/Akt signaling. J Biol Chem. 2018 Jun 8;293(23):9113–23.

28. Repnik U, Borg Distefano M, Speth MT, Ng MYW, Progida C, Hoflack B, et al. L-leucyl-L-leucine methyl ester does not release cysteine cathepsins to the cytosol but inactivates them in transiently permeabilized lysosomes. J Cell Sci. 2017 Sep 15;130(18):3124–40.

29. Xu L, Shen X, Bryan A, Banga S, Swanson MS, Luo ZQ. Inhibition of host vacuolar H+-ATPase activity by a Legionella pneumophila effector. PLoS Pathog. 2010 Mar 19;6(3):e1000822.

30. Sprouffske K, Wagner A. Growthcurver: an R package for obtaining interpretable metrics from microbial growth curves. BMC Bioinformatics. 2016 Apr 19;17:172.

31. O'Neill AM, Thurston TLM, Holden DW. Cytosolic Replication of Group A Streptococcus in Human Macrophages. mBio. 2016 Apr 12;7(2):e00020-00016.

32. Bright NA, Davis LJ, Luzio JP. Endolysosomes Are the Principal Intracellular Sites of Acid Hydrolase Activity. Curr Biol CB. 2016 Sep 12;26(17):2233–45.

33. Canton J, Grinstein S. Chapter 5 - Measuring lysosomal pH by fluorescence microscopy. In: Platt F, Platt N, editors. Methods in Cell Biology [Internet]. Academic Press; 2015 [cited 2021 Jul 1]. p. 85–99. (Lysosomes and Lysosomal Diseases; vol. 126). Available from: https://www.sciencedirect.com/science/article/pii/S0091679X14000223

34. Degnan BA, Fontaine MC, Doebereiner AH, Lee JJ, Mastroeni P, Dougan G, et al. Characterization of an isogenic mutant of Streptococcus pyogenes Manfredo lacking the ability to make streptococcal acid glycoprotein. Infect Immun. 2000 May;68(5):2441–8.

35. Cusumano ZT, Caparon MG. Citrulline protects Streptococcus pyogenes from acid stress using the arginine deiminase pathway and the F1Fo-ATPase. J Bacteriol. 2015 Apr;197(7):1288–96.

36. Maudsdotter L, Jonsson H, Roos S, Jonsson AB. Lactobacilli reduce cell cytotoxicity caused by Streptococcus pyogenes by producing lactic acid that degrades the toxic component lipoteichoic acid. Antimicrob Agents Chemother. 2011 Apr;55(4):1622–8.

37. Daglia M, Papetti A, Grisoli P, Aceti C, Dacarro C, Gazzani G. Antibacterial activity of red and white wine against oral streptococci. J Agric Food Chem. 2007 Jun 27;55(13):5038–42.

38. Jin H, Agarwal S, Agarwal S, Pancholi V. Surface export of GAPDH/SDH, a glycolytic enzyme, is essential for Streptococcus pyogenes virulence. mBio. 2011;2(3):e00068-00011.

39. Cotter PD, Hill C. Surviving the acid test: responses of gram-positive bacteria to low pH. Microbiol Mol Biol Rev MMBR. 2003 Sep;67(3):429–53, table of contents.

40. Molloy EM, Cotter PD, Hill C, Mitchell DA, Ross RP. Streptolysin S-like virulence factors: the continuing sagA. Nat Rev Microbiol. 2011 Sep;9(9):670–81.

41. Shaughnessy LM, Hoppe AD, Christensen KA, Swanson JA. Membrane perforations inhibit lysosome fusion by altering pH and calcium in Listeria monocytogenes vacuoles. Cell Microbiol. 2006 May;8(5):781–92.

42. Ambati J, Canakis CS, Miller JW, Gragoudas ES, Edwards A, Weissgold DJ, et al. Diffusion of high molecular weight compounds through sclera. Invest Ophthalmol Vis Sci. 2000 Apr;41(5):1181–5.

43. Cheng YL, Wu YW, Kuo CF, Lu SL, Liu FT, Anderson R, et al. Galectin-3 Inhibits Galectin-8/Parkin-Mediated Ubiquitination of Group A Streptococcus. mBio. 2017 Jul 25;8(4):e00899-17.

44. O'Seaghdha M, Wessels MR. Streptolysin O and its co-toxin NAD-glycohydrolase protect group A Streptococcus from Xenophagic killing. PLoS Pathog. 2013;9(6):e1003394.

45. Cusumano ZT, Watson ME, Caparon MG. Streptococcus pyogenes arginine and citrulline catabolism promotes infection and modulates innate immunity. Infect Immun. 2014 Jan;82(1):233–42.

46. Keyel PA, Roth R, Yokoyama WM, Heuser JE, Salter RD. Reduction of streptolysin O (SLO) pore-forming activity enhances inflammasome activation. Toxins. 2013 Jun 6;5(6):1105–18.

47. Chu J, Thomas LM, Watkins SC, Franchi L, Núñez G, Salter RD. Cholesterol-dependent cytolysins induce rapid release of mature IL-1beta from murine macrophages in a NLRP3 inflammasome and cathepsin B-dependent manner. J Leukoc Biol. 2009 Nov;86(5):1227–38.

48. Richter J, Monteleone MM, Cork AJ, Barnett TC, Nizet V, Brouwer S, et al. Streptolysins are the primary inflammasome activators in macrophages during Streptococcus pyogenes infection. Immunol Cell Biol. 2021 Nov;99(10):1040–52.

49. LaRock DL, Russell R, Johnson AF, Wilde S, LaRock CN. Group A Streptococcus Infection of the Nasopharynx Requires Proinflammatory Signaling through the Interleukin-1 Receptor. Infect Immun. 2020 Sep 18;88(10):e00356-20.

50. Campden RI, Zhang Y. The role of lysosomal cysteine cathepsins in NLRP3 inflammasome activation. Arch Biochem Biophys. 2019 Jul 30;670:32–42.

51. Kim ML, Martin WJ, Minigo G, Keeble JL, Garnham AL, Pacini G, et al. Dysregulated IL-1β-GM-CSF Axis in Acute Rheumatic Fever That Is Limited by Hydroxychloroquine. Circulation. 2018 Dec 4;138(23):2648–61.

52. Cortés G, Wessels MR. Inhibition of dendritic cell maturation by group A Streptococcus. J Infect Dis. 2009 Oct 1;200(7):1152–61.

10 Tables

Table 1: Final pH of media after bacterial growth, mean ± SD

starting pH	4.0	5.0	6.0	7.0	media (6.6)
ending pH	4.10 ± 0.02	5.07 ± 0.02	4.99 ± 0.01	5.23 ± 0.08	5.63 ± 0.06

11 Figure legends

Figure 1: GAS persists in phagolysosomes of THP-1 cells. THP-1 cells were infected with GAS for the indicated times, fixed and probed with anti-LAMP-1 (green) and anti-human IgG (bacteria, red) antibodies. **(A)** Representative image of LAMP-1 colocalized with GAS in THP-1 cells at 60 min. post-infection. Arrowheads indicate examples of colocalization. **(B)** Quantitation of LAMP-1 positive bacteria at the indicated time points. **(C)** Average number of bacteria per cell at the indicated time points. For all graphs, data from three independent experiments were combined and results are given as mean ± 95% CI. Data were analyzed by one-way ANOVA with Tukey's multiple comparisons test.

Figure 2: GAS persists in non-acidified phagolysosomes of THP-1 cells. (A) GAS expressing mWASABI were incubated at the indicated pH. Representative green fluorescence (mWASABI) and brightfield images are shown. **(B)** Corrected total cell fluorescence of green fluorescence signal from bacteria expressing mWASABI incubated at the indicated pH for 1 hour. **(C)** Representative fluorescence microscopy images of GAS-infected THP-1 cells at 7.5 and 60 min. post-infection. Arrowheads denote examples of bacteria encapsulated in early phagosomes (EEA-1, magenta), arrows denote examples of bacteria encapsulated in phagolysosomes (LAMP-2, red). Fluorescence

images merged with brightfield images are shown in the bottom row. All images were taken with a 63x objective with 2x digital zoom. **(D)** Quantitation of bacteria colocalized with phagosomes (EEA-1) or phagolysosomes (LAMP-2) at the indicated time points. **(E)** Average number of bacteria per cell at the indicated time points. **(F)** Violin plot of fluorescence signal intensity from intracellular (clear bars) or extracellular (shaded bars) bacteria expressing mWASABI. **(G)** Fluorescence signal from cells fed 70kD FITC dextran and infected with immunoglobulin-conjugated beads (Ab beads), the indicated GAS strain or heat-killed (HK) bacteria. Significance indicates difference from Ab beads (positive control). Data from at least three independent experiments were combined. For (D) and (E), data from 5 individual counters of three independent experiments were combined. Results are given as mean ± 95% CI and analyzed by one-way ANOVA with Kruskal-Wallis multiple comparison test.

Figure 3: GAS does not survive in low pH environments. (A) Growth curves of bacteria grown in buffered media or unbuffered bacterial media (THB) at the indicated pH. Results are given as mean ± 95% CI. Statistics in (A) indicate differences in intrinsic growth rate compared with bacteria grown in unbuffered media. **(B)** Bacterial survival in buffered media at the indicated pH compared with survival of bacteria in unbuffered bacterial media (THB). Results are given as mean ± SEM. Statistics in (B) are shown only for pH = 4.9 and 5.3 media and indicate differences in bacterial survival at the corresponding time point compared with bacteria in unbuffered media. Differences for bacteria grown in pH = 4.7 or lower media were statistically significant compared with unbuffered media at all time points after 30 min. For each experiment, samples were prepared in triplicate and data from at least three independent experiments were combined.

Figure 4: SLO induces phagolysosomal perforation and protein leakage. (A) Representative images of the 40kD dextran probe (green) with indicated bacterial strains (magenta). Arrowheads indicate examples of colocalization. All images were taken with a 63x objective with 2x digital zoom. **(B)** Quantitation of colocalization of indicated bacterial strains with 10, 40 and 70kD dextran probes. Results are given as mean ± 95% CI and analyzed by one-way ANOVA with Tukey's multiple comparison test. **(C)** Cells were infected with the indicated bacterial strains, fractionated into membrane (left) and cytosolic (right) fractions, and probed with the indicated antibodies: LAMP-2 (lysosomal marker; loading control for membrane fraction), GAPDH (cytosolic marker; loading control for cytosolic fraction) and cathepsin B (lysosomal enzyme). **(D)** Cathepsin B activity was measured in cytosolic cell fractions collected from cells infected with the indicated strains. Data in (B) and (D) are combined from at least three independent experiments.

Figure 5: GAS infection limits v-ATPase activity. (A) Cells were infected with immunoglobulin-conjugated beads (Ab beads, control), the indicated GAS strain or heat-killed (HK) bacteria and fractionated into membrane (M) and cytosolic (C) fractions. Fractions were probed with antibodies to V_1A, V_0D or GAPDH proteins. Representative data are shown. **(B)** Quantitation of data shown in (A). V_1A band intensities were quantified and normalized to V_0D (membrane) or GAPDH (cytosol). Relative assembly was calculated as the amount of V_1A in the membrane fraction of the indicated infected sample compared with the uninfected sample for each experiment. **(C)** v-ATPase activity assay in membrane fractions from cells infected with the indicated GAS strain. Data in (B) and (C) are combined from at least three independent experiments and results are given as mean ± 95% CI and analyzed by one-way ANOVA with Tukey's multiple comparison test.

A

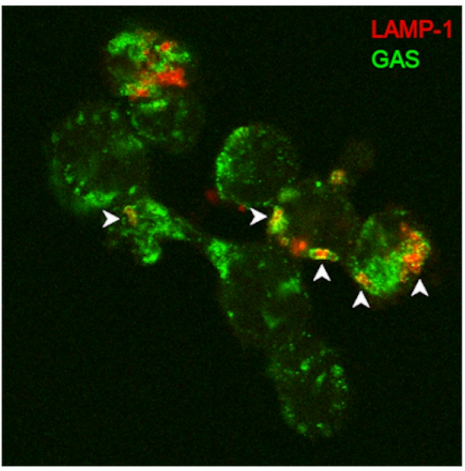

B

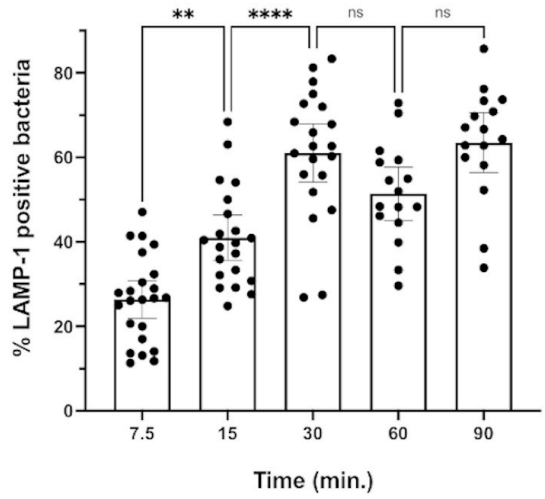

C

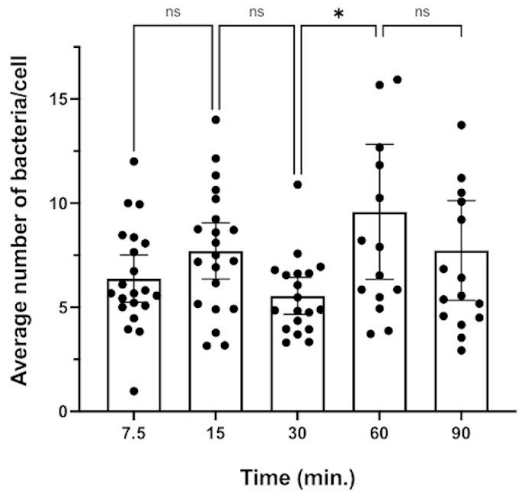

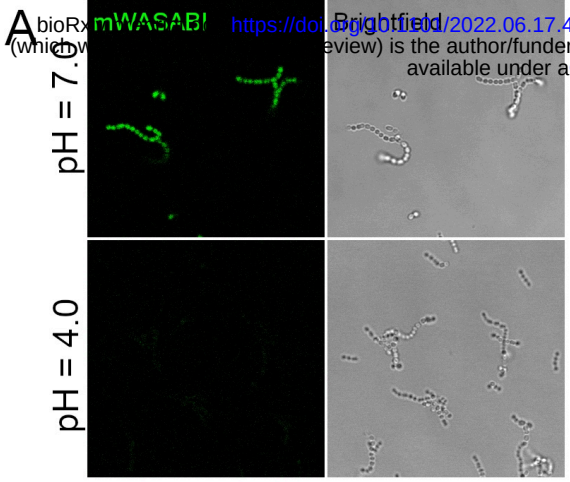

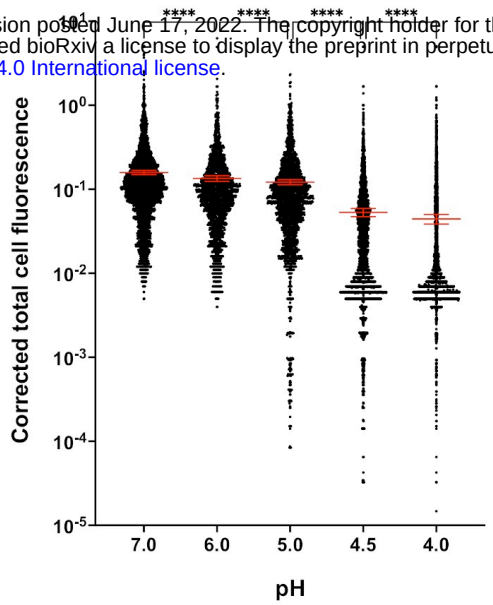

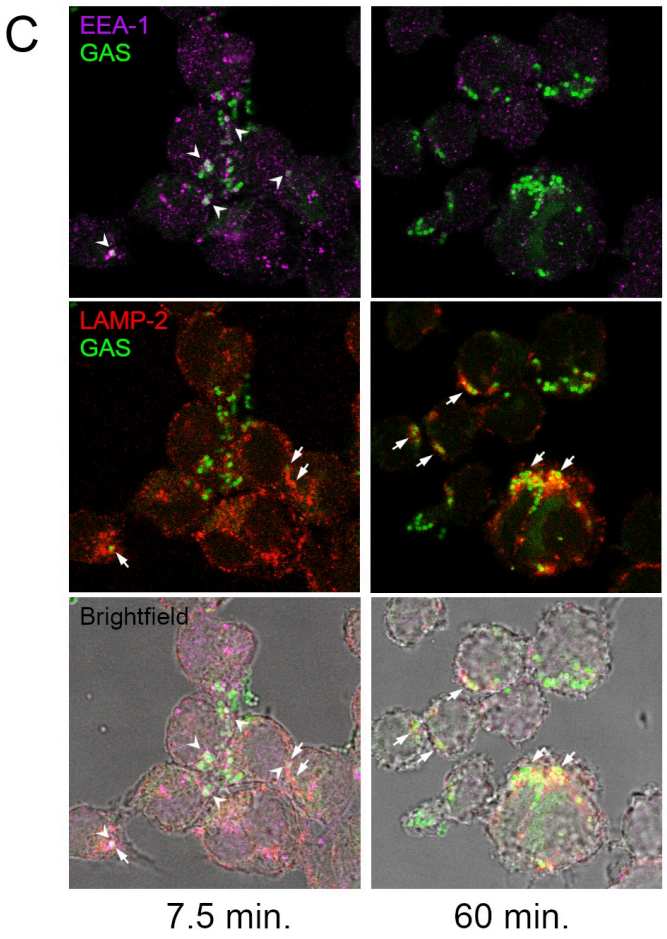

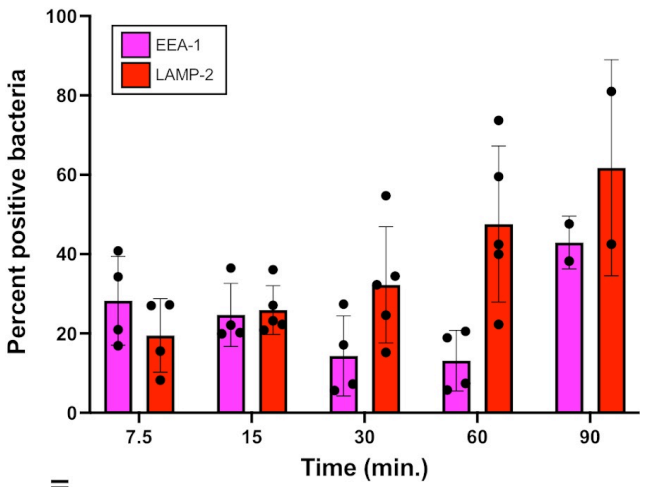

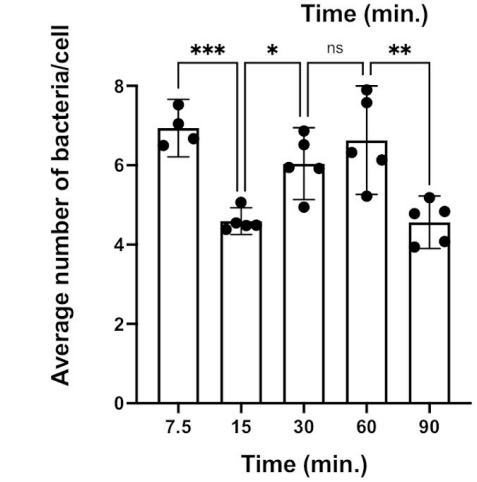

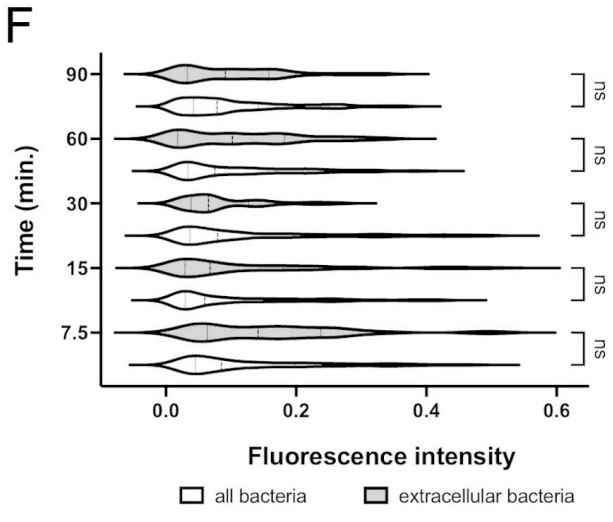

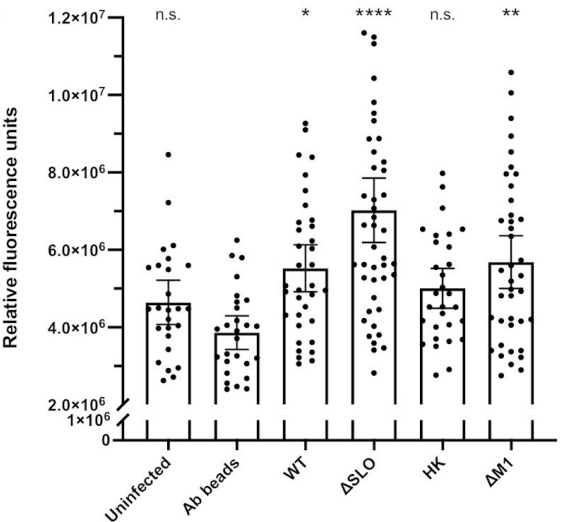

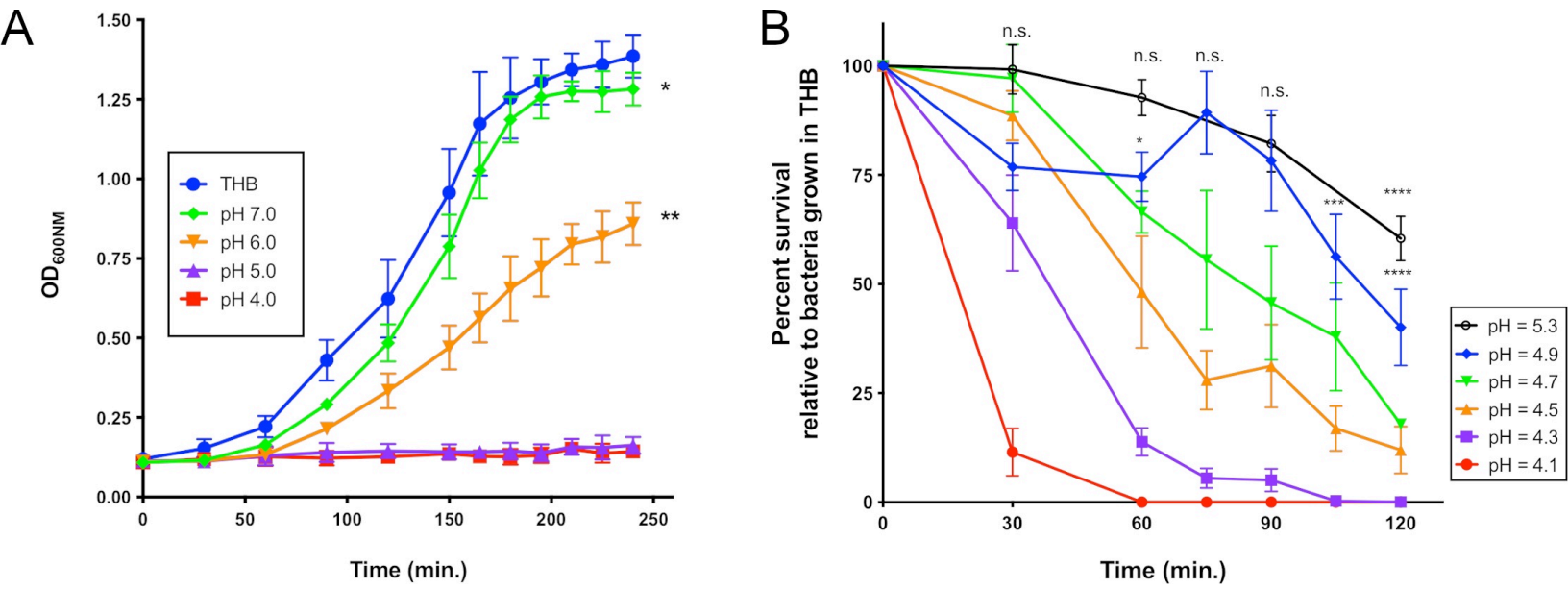

A

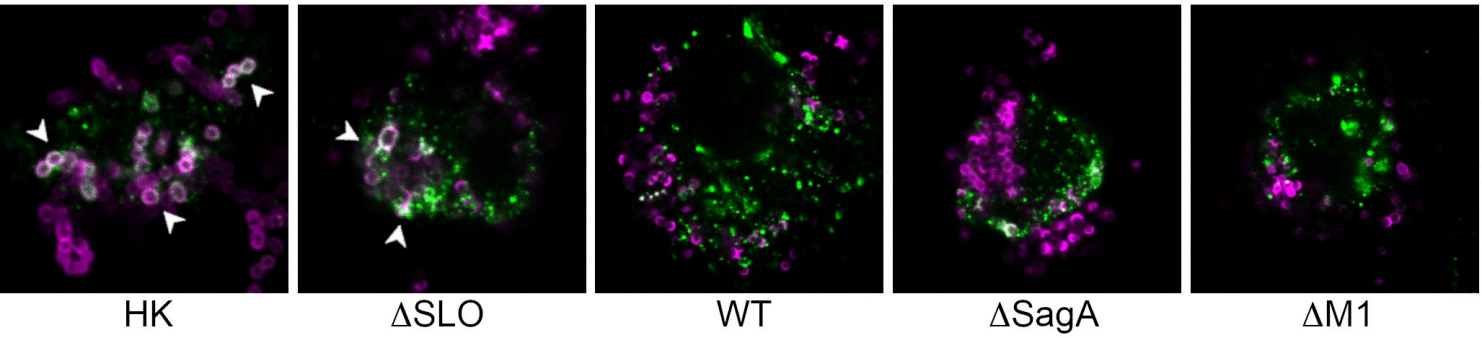

B

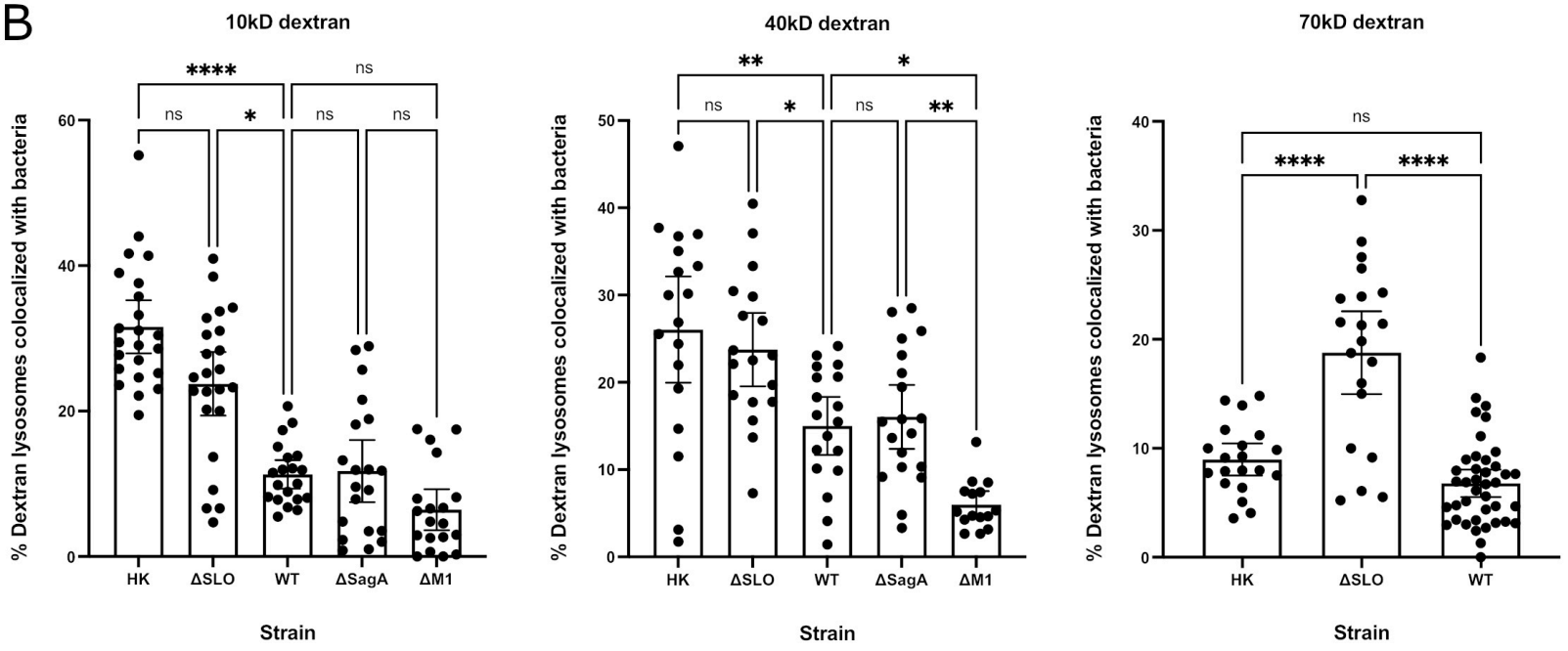

C

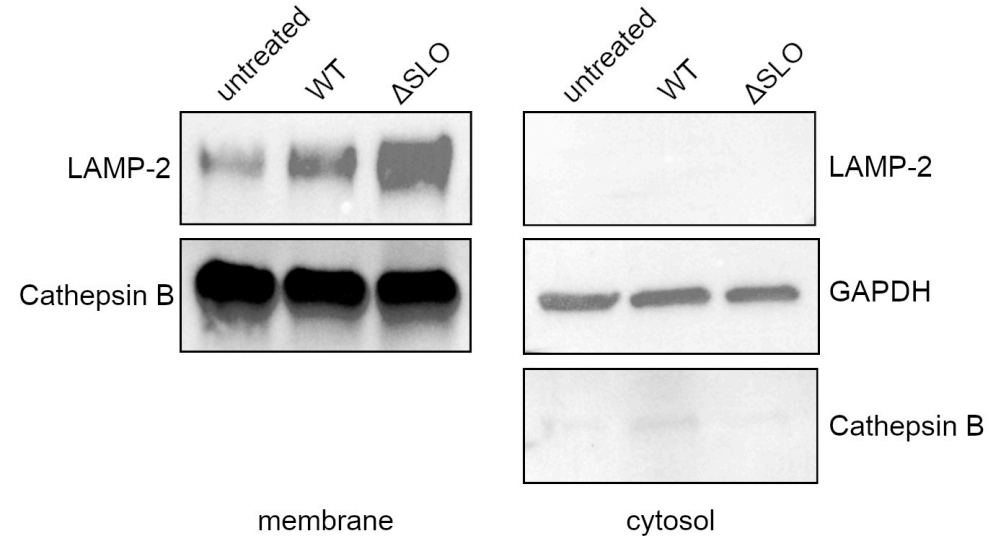

D

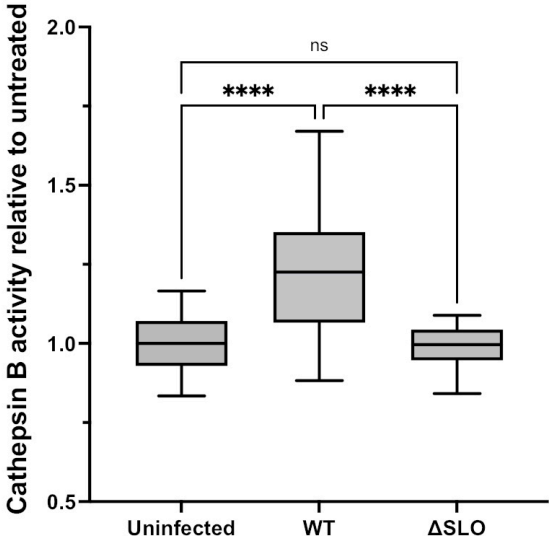

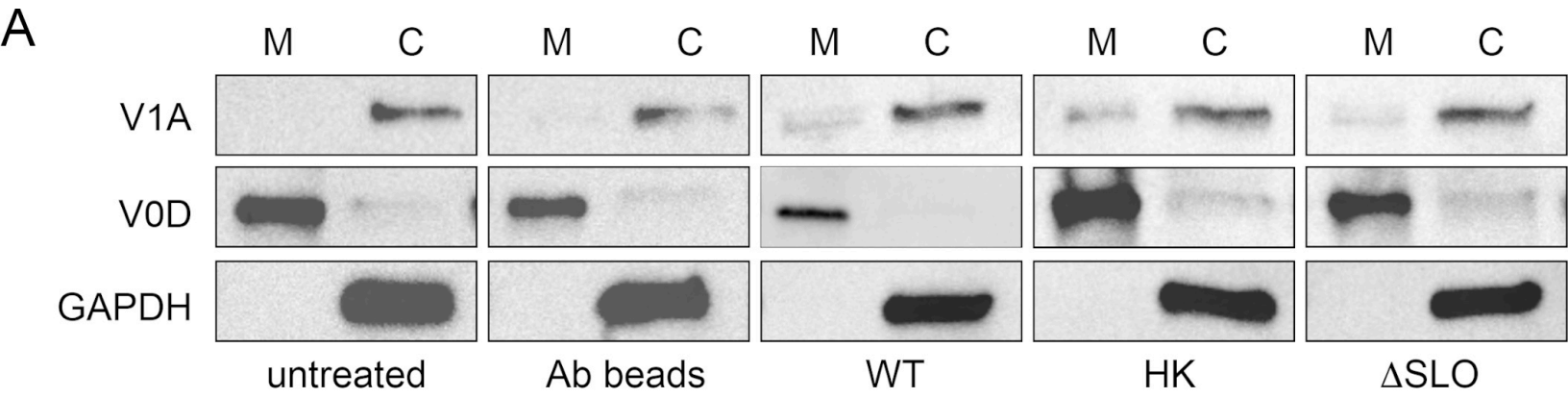

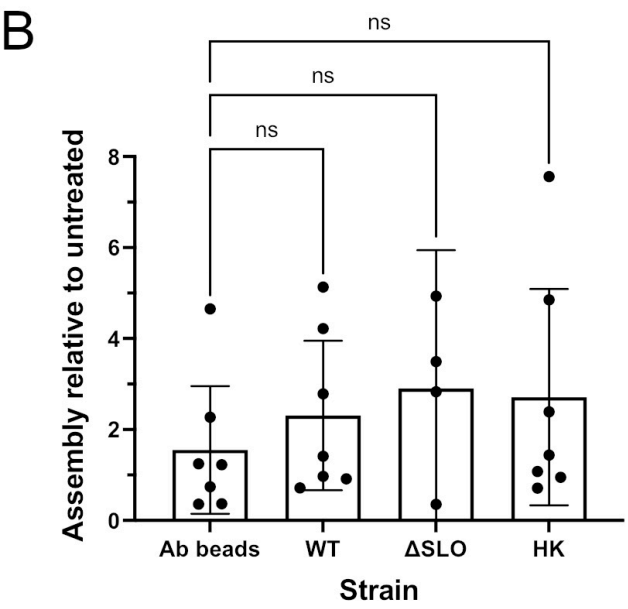

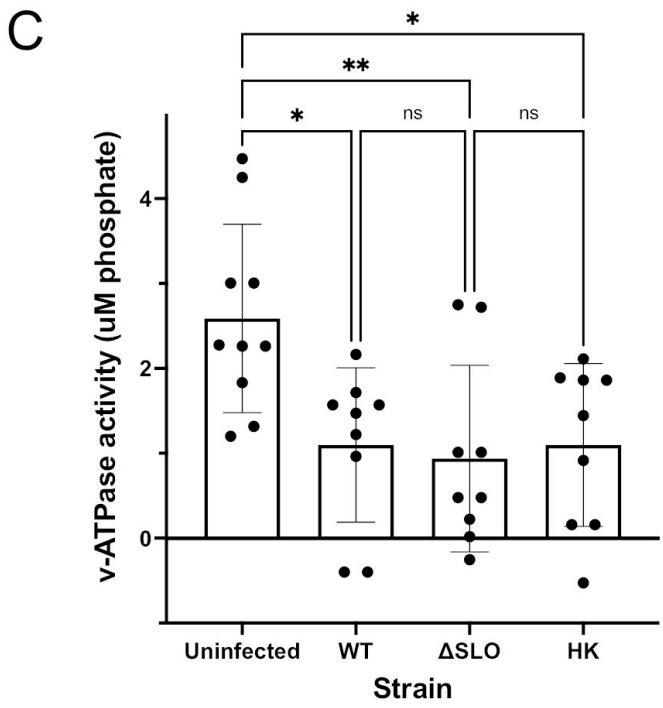

Supplementary Material

1 Supplementary Data

mWASABI amino acid sequence:

MVSKGEETTMGVIKPDMKIKLKMEGNVNGHAFVIEGEGEGKPYDGTNTINLEVKEGAPLPF
SYDILTTAFSYGNRAFTKYPDDIPNYFKQSFPEGYSWERTMTFEDKGIVKVKSDISMEEDSFI
YEIHLKGENFPPNGPVMQKETTGWDASTERMYVRDGVLKGDVKMKLLLEGGGHHRVDFK
TIYRAKKAVKLPDYHFVDHRIEILNHDKDYNKVTVYEIAVARNSTDGMDELYK

2 Supplementary Figures

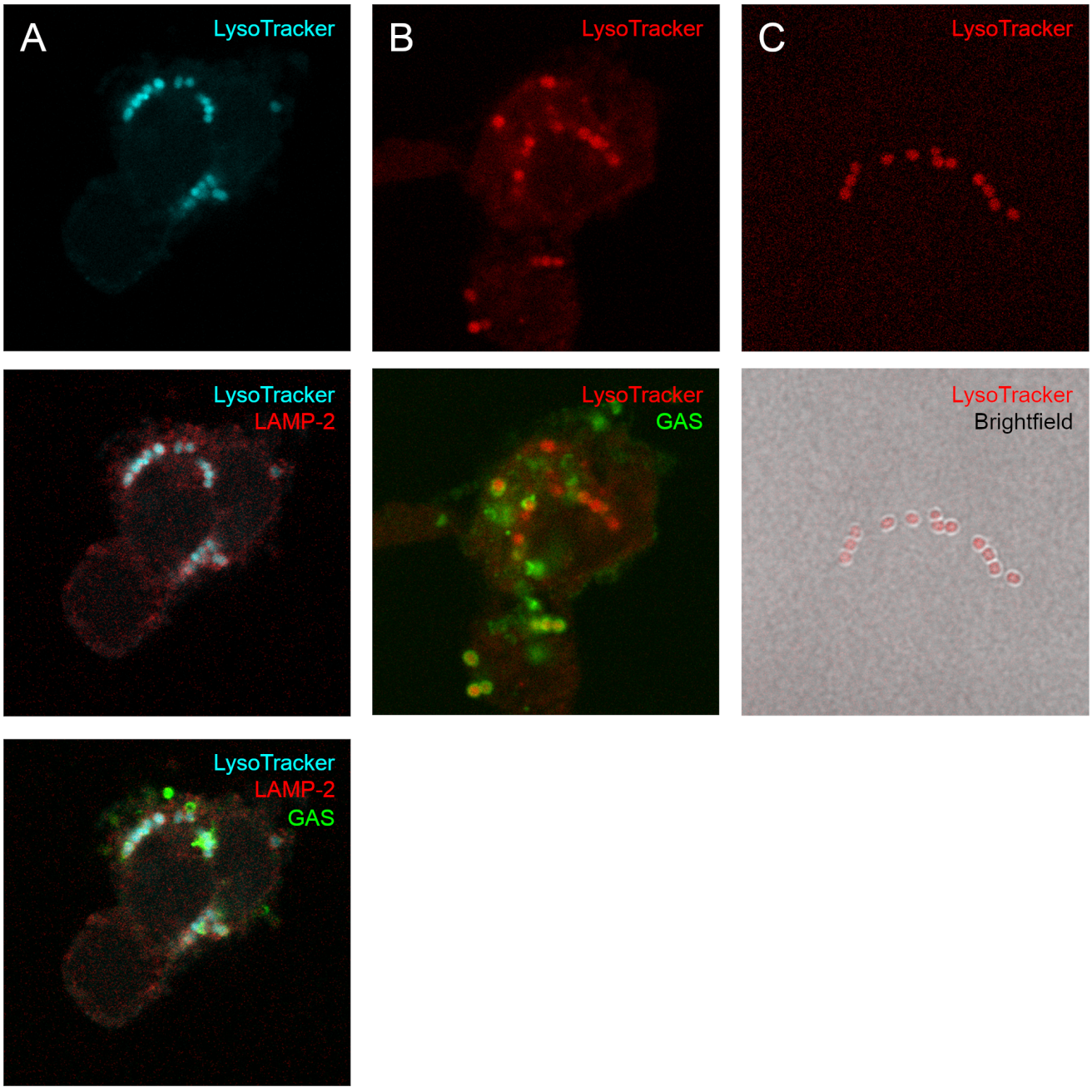

Supplemental Figure 1: Lysotracker detects GAS. Cells were loaded with 100nM LysoTracker Deep Red (Thermo Fisher Scientific) prior to infection and infected with GAS for 30 min. Cells were fixed and stained with LAMP-2 (lysosome) and anti-human IgG (bacteria) antibodies as indicated: **(A)** LysoTracker (blue), LAMP-2 (red), and GAS (green). **(B)** Lysotracker (red) and GAS (green). **(C)** Bacteria alone incubated with 100nM Lysotracker (red). All images were taken with a 63x objective with 2x digital zoom.

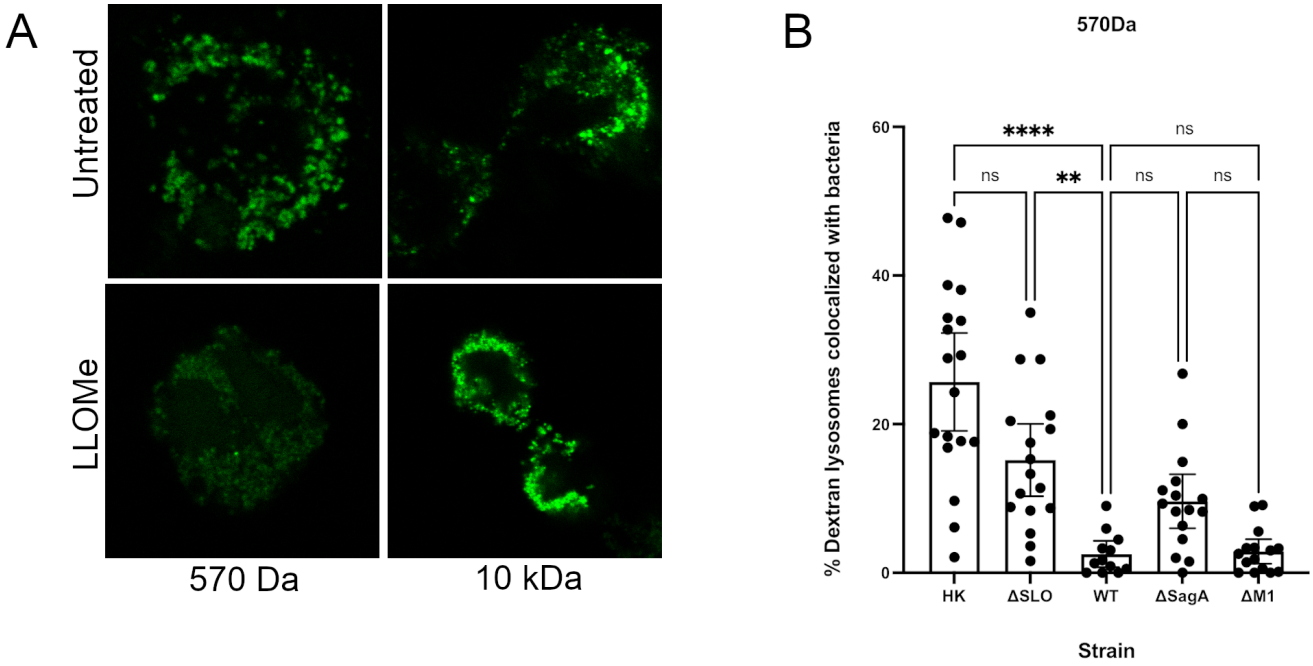

Supplemental Figure 2: Fluorescent probes appropriately monitor phagolysosomal leakage. Cells were loaded with Alexa-fluor 488 dye (570 Da) or 10kD Oregon Green dextran (10kDa) for 24 hrs., then either untreated, treated with 1mM LLOMe or infected with the indicated GAS strain. **(A)** Representative images of fluorescent probe-loaded cells in the presence or absence of LLOMe. All images were taken with a 63x objective with 2x digital zoom. **(B)** Quantitation of colocalization of Alexa-fluor 488 (570Da) with indicated bacterial strains. Data from three independent experiments were combined and are given as mean ± 95% CI.

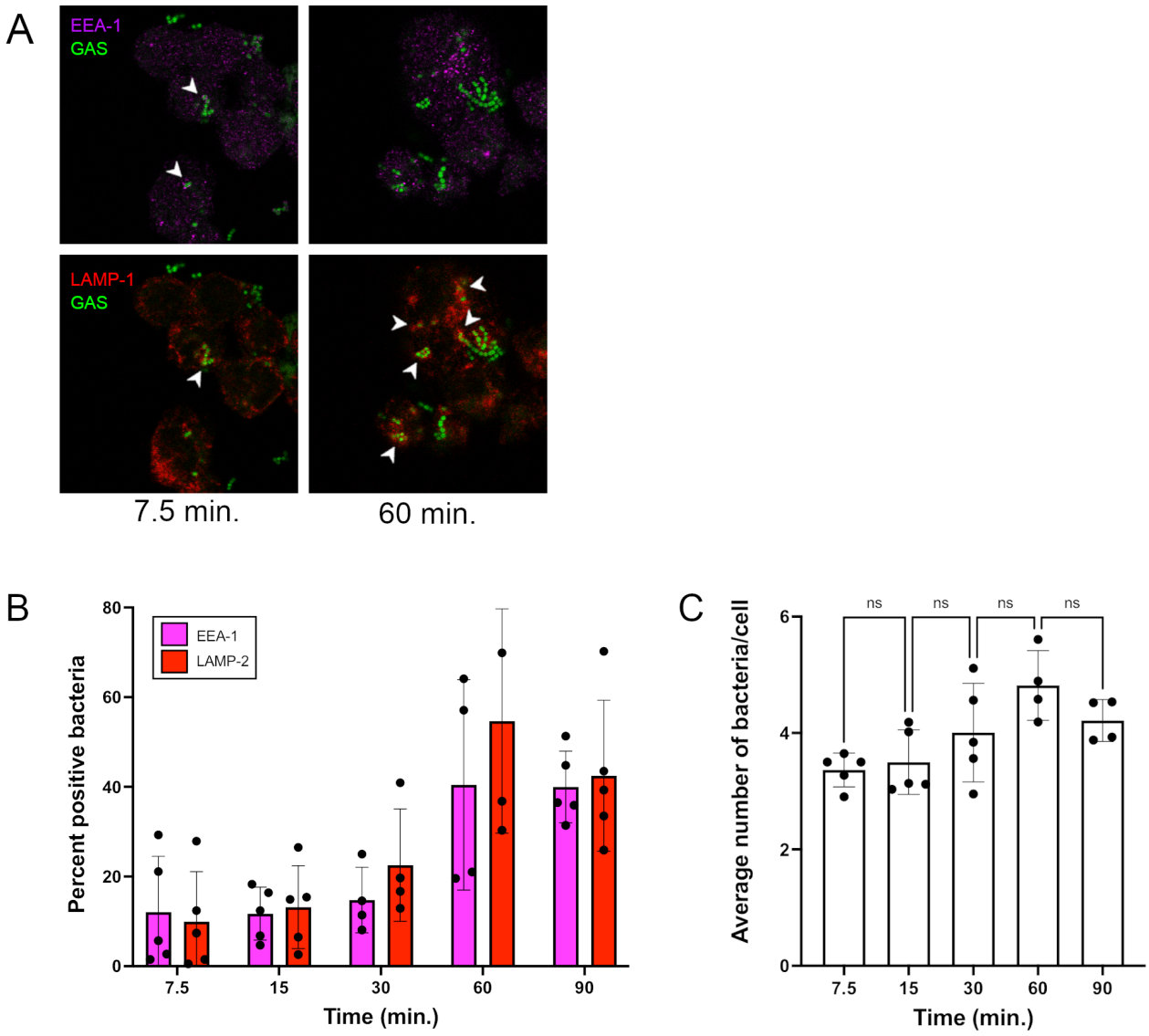

Supplemental Figure 3: ΔSLO GAS persist in THP-1 phagolysosomes. (A) Representative fluorescence microscopy images of ΔSLO-infected THP-1 cells at 7.5 and 60 min. post-infection. Arrowheads denote examples of ΔSLO bacteria (green) encapsulated in early phagosomes (EEA-1, magenta) or in phagolysosomes (LAMP-2, red). All images were taken with a 63x objective with 2x digital zoom. **(B)** Quantitation of bacteria in intracellular compartments. **(C)** Average number of bacteria per cell at the indicated time points. For B and C, data from at least 5 individual counters of three independent experiments were combined. Results are given as mean ± 95% CI and analyzed by one-way ANOVA with Kruskal-Wallis multiple comparison test.